Alkaline magmatism subsequent to collision in the Pan-African belt of the Adrar des Iforas (Mali)

J. P. Liégeois and R. Black

SUMMARY: The Pan-African Trans-Saharan belt in the Iforas displays a rapid switch from subduction and collision-related calc-alkaline to typical A-type magmatism, which is accompanied by transcurrent movements along major shear zones inducing weak distension. Detailed Rb–Sr geochronology and geochemical data point to different mantle sources for orogenic (lithospheric depleted mantle + oceanic crust) and within-plate magmatism (more primitive asthenospheric mantle). Both groups suffer lower-crustal contamination. A model is proposed whereby asthenospheric mantle originally underlying the subducted plate has risen to shallow depth beneath the continental lithosphere after the rupture of the cold plunging plate. This source, which is often proposed for alkaline rocks, explains the great similarity of oversaturated alkaline ring-complexes whatever their environment. The peculiarities of the alkaline province, for example the lack of Sn mineralization when compared with the Niger–Nigerian province, may be related to the nature and composition of the basement.

Introduction

The Cambrian saturated alkaline ring complexes of the Iforas (Ba *et al.* 1985) mark the end of the Pan-African, characterized here by oceanic closure around 600 Ma ago and oblique collision between the passive margin of the W African craton and the active margin of the Tuareg shield (Black *et al.* 1979; Caby *et al.* 1981; Fabre *et al.* 1982; Ball & Caby 1984). This post-tectonic setting contrasts with that of the anorogenic within-plate Niger–Nigeria province where there is a considerable lapse of time (several hundred million years) between the age of the country rocks and that of the alkaline intrusions (Black *et al.* 1985).

The aim of this paper is to outline very briefly the main structural and petrological characteristics of the Iforas alkaline province, to trace chronologically and geochemically the transition from calc-alkaline to alkaline magmatism and finally to propose a geodynamic model which may also fit other collisional terrains displaying similar magmatic sequences, e.g. Pan-African of Saudi Arabia (Duyvermann *et al.* 1982; Harris 1982), Permian of Corsica (Bonin 1980), Tertiary volcanism of the Turkish–Soviet Armenia–W Iranian Alpine segment (Innocenti *et al.* 1982) and the Basin and Range province (Eaton 1982).

General geology

Whereas the 2000 Ma old W African craton is simply covered by Upper Proterozoic and Phanerozoic flat-lying sediments, the adjacent Tuareg shield emerging from beneath Ordovician strata has a complex geological history with diversified and abundant igneous activity between 850 and 530 Ma ago. These features are best explained by a complete Wilson cycle in Pan-African times.

After rifting around an RRR triple junction in the Gourma area (Moussine-Pouchkine & Bertrand-Sarfati 1978) followed by oceanic spreading to the E of the W African craton, a long period of subduction (720–620 Ma) is recorded in the Iforas along the SW margin of the Tuareg shield (Ducrot *et al.* 1979; Caby *et al.*, 1986. The subduction-related magmatism over an easterly-dipping Benioff plane appears in two environments: an oceanic trench island arc to the W of the Iforas (Caby 1970, 1981) and a cordilleran assemblage with andesites in the Iforas (Chikhaoui 1981). Oceanic closure and collision occurred 620–590 Ma ago, the suture between the W African craton and the Tuareg shield being marked by an array of strong positive gravity anomalies (Bayer & Lesquer 1978). Collision was not frontal as in the Himalaya but oblique (Ball & Caby 1984), inducing N–S mega-shear zones which sliced the Iforas and absorbed part of the collision. Nappes, comprising elements of the passive continental margin, oceanic basalts, possible ophiolites and an inner unit of eclogitic mica schists, were translated westward onto the W African craton (Caby 1980). This craton behaved as a relatively rigid mass devoid of autochtonous Pan-African magmatism, in contrast with the active margin of the Tuareg shield which was strongly mobilized and invaded by abundant granitoids which form a huge composite late-tectonic calc-alkaline batholith 100–150 km to the E of the suture. The calc-alkaline manifestations continued in post-tectonic condi-

From: FITTON, J. G. & UPTON, B. G. J. (eds), 1987, *Alkaline Igneous Rocks*, Geological Society Special Publication No. 30, pp. 381–401.

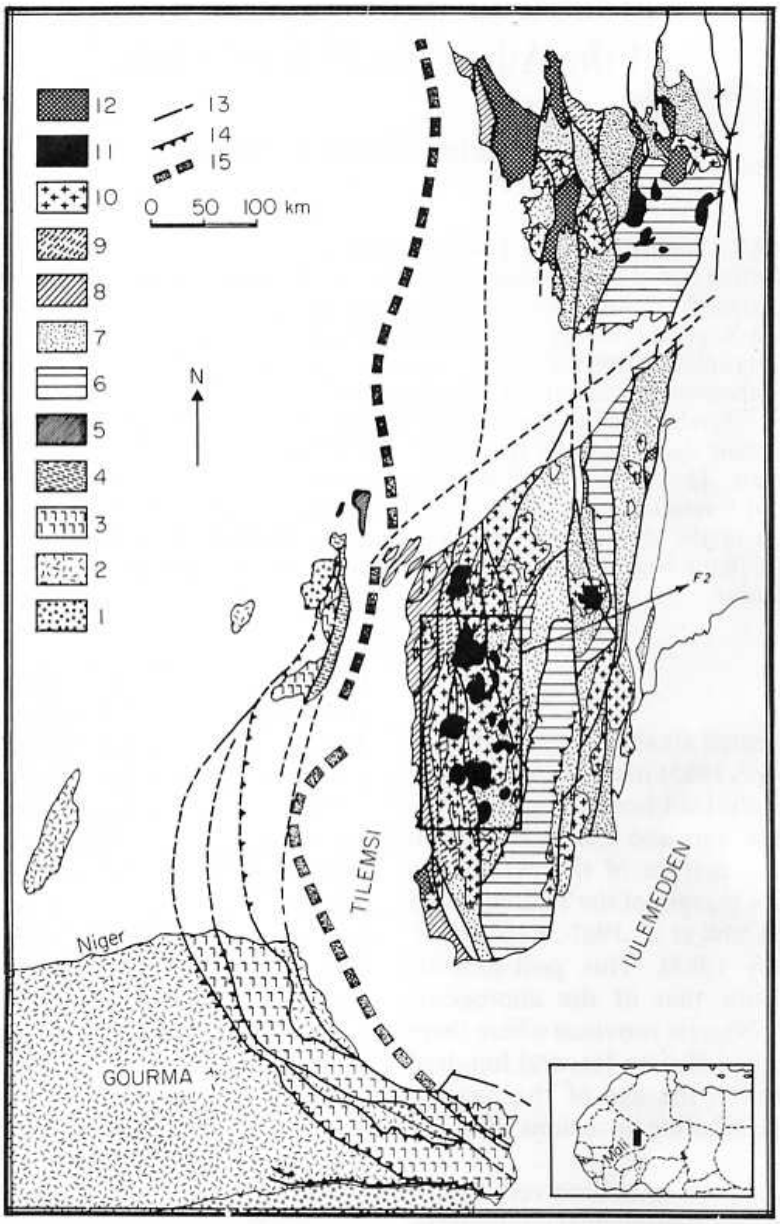

FIG 1. Structural map of the Iforas–Ahnet area (1–5, passive margin of the W African craton; 6–12; active margin of the Iforas): 1, Eburnean unreactivated basement; 2, autochthonous passive margin (Gourma aulacogen); 3, Timetrine–Gourma nappes; 4, Permian Tessofi graben; 5, Permian Tadhak undersaturated ring-complexes province; 6, Eburnean granulites (Archaean substratum?); 7, reactivated basement; 8, island arc; 9, cordilleran volcano–sedimentary unit; 10, composite calc-alkaline batholith; 11, oversaturated alkaline ring-complexes and lavas; 12, Cambrian molasse; 13, transcurrent faults; 14, thrusts; 15, suture zone as indicated by a string of positive gravity anomalies; F2, area of Fig. 2. (After Fabre *et al.* 1982.)

tions with WNW–ESE dyke-swarms and high-level circular plutons which indicate uplift of the continent subsequent to collision. This uplift led to unroofing the batholith just after the emplacement of the first granite displaying some alkaline affinities (Tahrmert). Renewed intermittent movements along the N–S shear zones and a change in the stress field was accompanied by the injection of spectacular N–S dyke-swarms in the axis of the batholith, feeding extensive plateaux of rhyolites and ignimbrites beneath which were emplaced the alkaline ring-complexes.

The Iforas alkaline province

The Cambrian alkaline province is superimposed on the Pan-African composite calc-alkaline batholith of Western Iforas. It comprises remnants of an extrusive cover of rhyolites and ignimbrites of fissural origin (Tiralrar, Ichoualen plateaux), dense N–S-oriented acid dyke-swarms and over 15 plutons displaying a variety of intrusion forms including huge ring-complexes, crescentic sheeted intrusions and sub-circular stocks. Contacts with the country rocks and between succes-

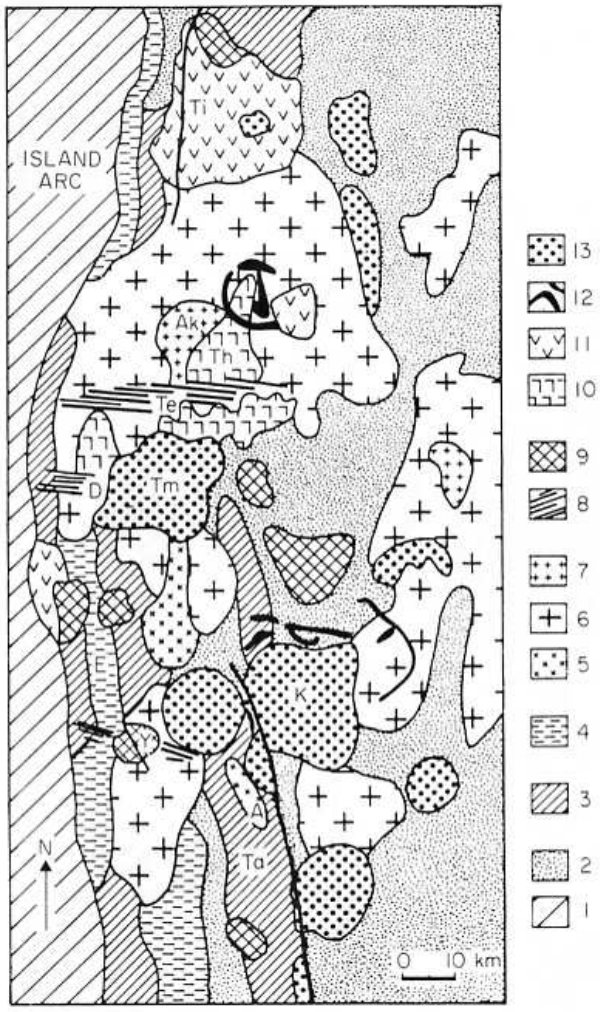

FIG. 2. Schematic map of the studied Kidal–Tiralrar area: 1, island arc; 2, reactivated basement; 3, volcano-sedimentary sequences; 4, pre-tectonic tonalite; 5, late-tectonic granodiorite; 6, late-tectonic porphyritic monzogranite; 7, late-tectonic fine-grained monzogranite; 8, post-tectonic E–W dyke-swarms; 9, post-tectonic syenogranite; 10, post-tectonic alkaline granite pluton; 11, extrusive alkaline rhyolites and ignimbrites; 12, syenitic ring-dykes; 13, alkaline oversaturated ring-complexes. For clarity, N–S dykes have not been drawn. (See Fig. 3.)

sive phases are sharp and typically show a chilled marginal facies with frequent development of miarolitic cavities. All the complexes have been emplaced at shallow depth in a rigid environment beneath a thick volcanic cover by a process of subterranean cauldron subsidence and major stoping. They are composed of typical A-type quartz syenites and granites (Loiselle & Wones 1979) embracing metaluminous, peralkaline and peraluminous compositions. The province is exclusively oversaturated and quite distinct from the much younger Permian Tadhak province of undersaturated alkaline rocks and carbonatites located on the eastern margin of the W African craton (Fig. 1) (Liégeois *et al.* 1983; Sauvage & Savard 1985).

A general description of the Iforas alkaline province has recently been published (Ba *et al.* 1985). Only a brief description of the units studied in this paper (Fig. 2) is given here, followed by a summary of the main geochemical and petrological features of the province.

The plateau lavas occurring as thick flows of devitrified and often altered rhyolites and ignimbrites have not been studied in detail. Inside the Ichoualen ring structure they are seen to overlie the eroded Tahrmert granite, a large irregular-shaped massif characterized by pronounced horizontal jointing which invades the Telabit and Dohendal WNW–ESE dyke-swarms to the N and W of the Timedjelalen ring-complex (Fig. 3). This coarse-grained hypersolvus granite already displays distinct alkaline affinities and, with its clustered rounded quartzes, perthites and abundant accessory minerals (zircon, Fe-Ti oxides, sphene and fluorite), it closely resembles some of the metaluminous biotite granites of the alkaline ring-complexes. The mafic minerals (brown phlogopitic biotite and occasional pale-blue richterite) are magnesian, however, and suggest that this alkaline precursor has a mixed source (Ba *et al.* 1985).

The N–S dykes are mainly composed of devitrified and often altered rhyolites, felsites and quartz–feldspar porphyries (believed to be feeders to the plateau rhyolites), quartz microsyenites often containing basic xenoliths, porphyry granites and granophyres. Both metaluminous and peralkaline varieties are present. Basic dykes are rare and have only been encountered to the N of Tiralrar.

Among the ring-complexes, the Kidal massif (Figs 3 and 4) with a diameter of 30 km is the largest and most intricate. It has been segmented and offset by a NNW sinistral transcurrent fault. The early arcuate ramified and polygonal ring-dykes of quartz syenite (K1) are partly obliterated by the plutonic centre which comprises 13 granitic phases whose order of intrusions is indicated in the legend of Fig. 4. A coarse hypersolvus granite (K3), displaying both metaluminous and peralkaline facies with related granite porphyries (K2–K3′), occurs as a flat tabular sheet covering two-thirds of the area and constitutes the upper structural level of the complex. It is thought to have intruded permissively a long and sub-horizontal tensional roof fracture fed by a peripheral ring-dyke. Granite porphyry (K4) marks the fragmentation of the underlying block and the start of an aluminous cycle with the emplacement of metaluminous hypersolvus granite (K5–K5′) followed by subsolvus granite (K6–

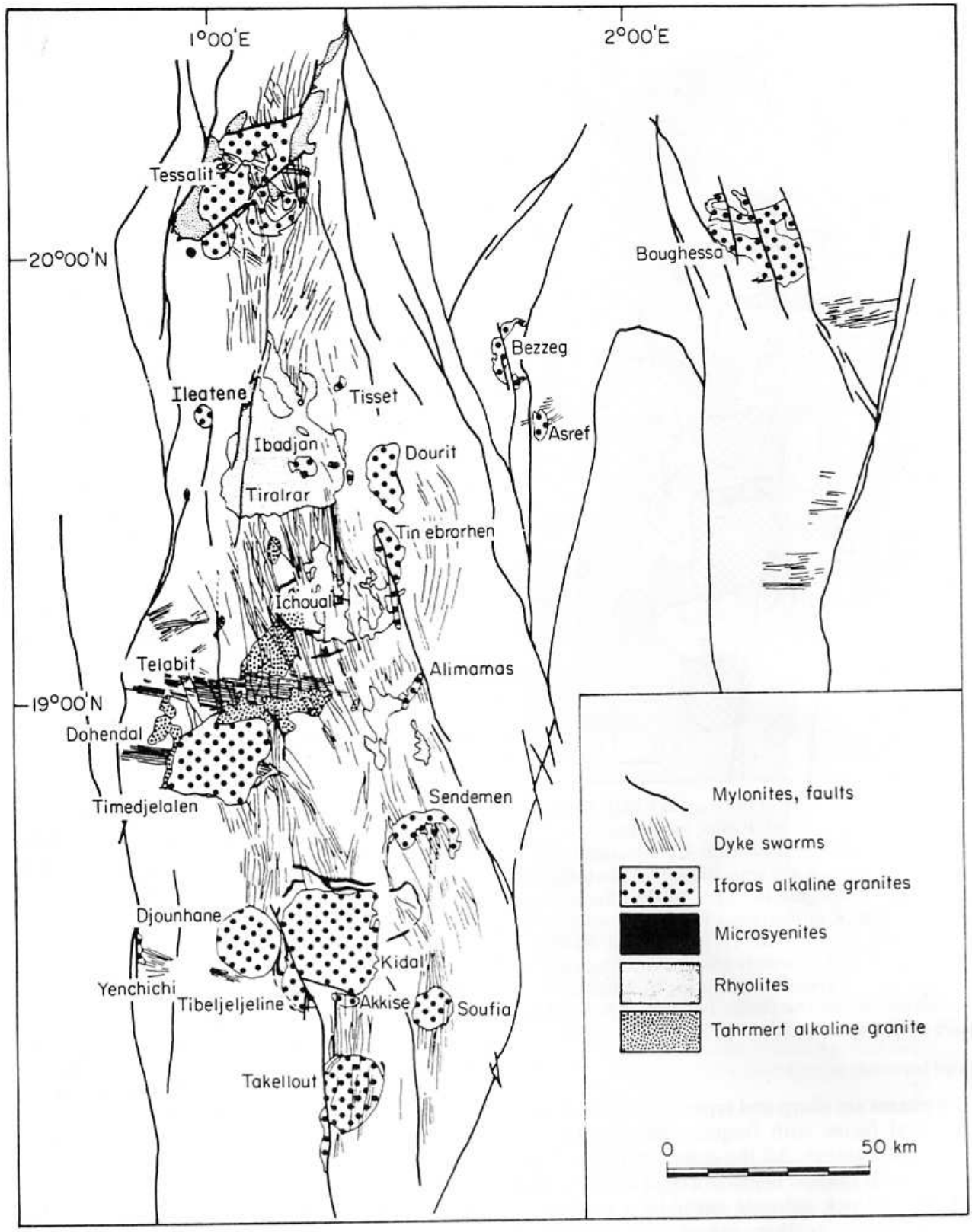

FIG. 3. Geological map of the Iforas alkaline province (Ba *et al.* 1985).

K8) and the late granite porphyry (K9) which defines several centres of subsidence. Magmatic activity is then confined to central and eastern parts of the complex with the intrusion beneath K3 and K7 of a peralkaline medium-grained granite (K10) which in turn is underlain by a metaluminous coarse-grained hypersolvus granite (K11) and by albitized peralkaline granite (K12) mineralized in Th minerals. The general shape of the massif has been confirmed by a gravity study (Ly *et al.* 1984) which indicates that the alkaline granites in the western part of the

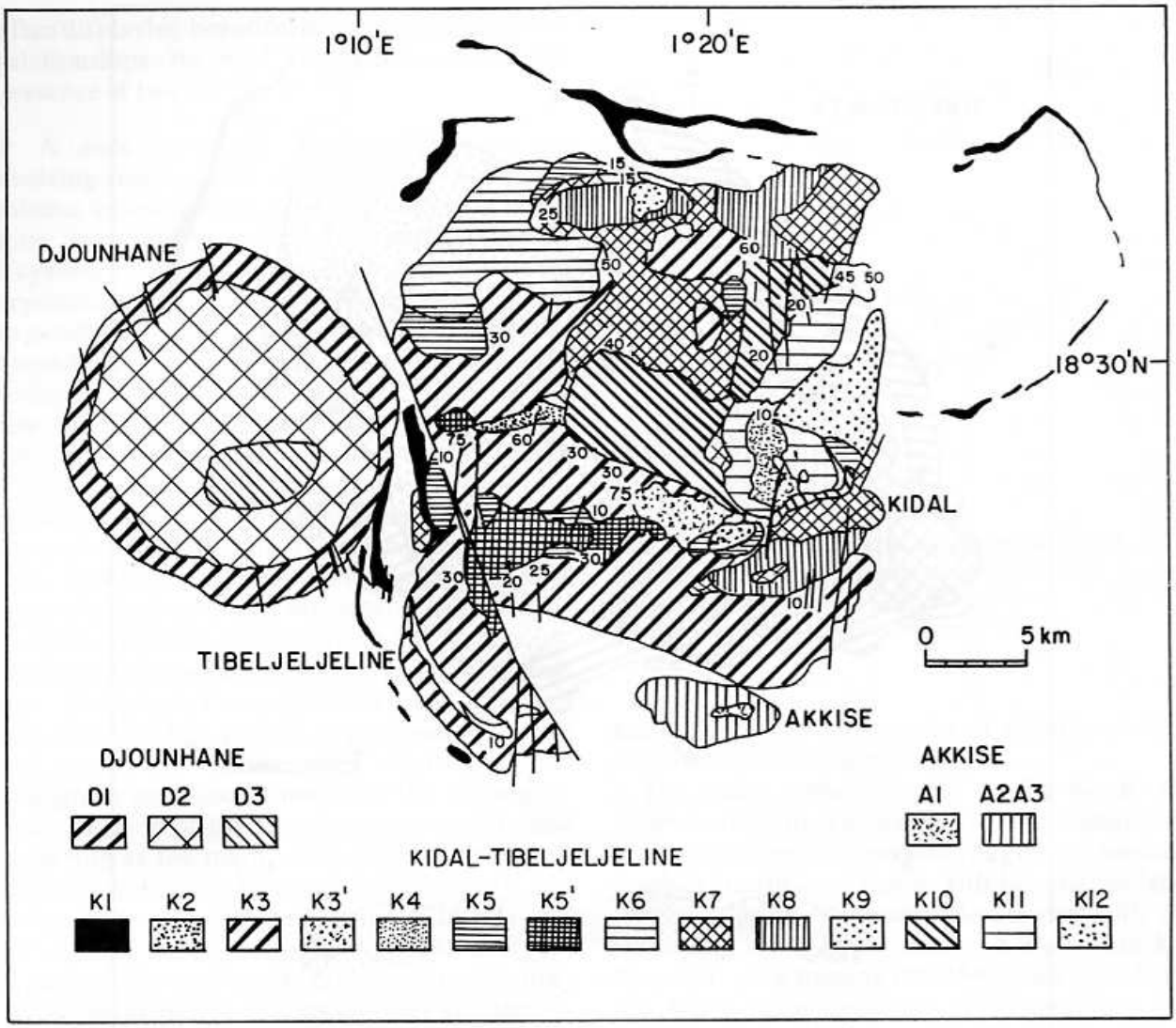

FIG. 4. Geological map of the Kidal–Tibeljelejeline, Djounhane and Akkise ring-complexes: K1, syenite porphyry and quartz syenite (Fe-augite, amphibole, biotite, ± fayalite); K2, amphibole–biotite granite porphyry; K3, metaluminous coarse-grained granite (perthite, hedenbergite, amphibole, biotite, ± fayalite) to peralkaline (perthite, aegirine–augite, Ca-Na- and Na-amphiboles, ± aenigmatite); K3′, peralkaline granite porphyry; K4, metaluminous granite porphyry (K-feldspar, hedenbergite, amphibole, biotite and two feldspars, amphibole, biotite); K5, fine-grained granite (perthite, biotite, chlorite, ± amphibole); K5′, medium-grained granite (perthite, amphibole, biotite, ± fayalite); K6, fine-grained granite (perthite, oligoclase, amphibole, biotite); K7, fine- to coarse-grained granite (perthite, oligoclase, amphibole, biotite); K8, fine-grained granite (perthite, oligoclase, biotite, chlorite); K9, granite porphyry (perthite, oligoclase, biotite, chlorite); K10, metaluminous medium-grained granite (hedenbergite, aegirine–augite, Fe-richterite, arvfedsonite, biotite) to peralkaline (aegirine, arvfedsonite, astrophyllite); K11, coarse-grained granite (perthite, amphibole, biotite); K12, fine-grained granite (microcline, albite, aegirine, Ca-Na- amphibole and microcline, albite, arfvedsonite); A1 = K2; A2 = K8; A3, granite porphyry (perthite, oligoclase, amphibole, biotite); D1 ≡ K3; D2 ≡ K7; D3 ≡ K8. (Ba *et al.* 1985).

complex are thin compared with those in the E which have been estimated to have a thickness of 5 km.

In contrast, the Timedjelalen ring-complex (Figs 3 and 5), with six concentrically disposed units younging towards the centre, is relatively simple despite its large size (32 km × 22 km). The sequence (see legend to Fig. 5) starts with mildly-peralkaline quartz-poor granite porphyry (T1) and medium-grained hypersolvus granite (T2) which form the steeply-dipping external ring-dyke injected in a multiple-fracture zone. Foundering of a central block permitted the emplacement of a peralkaline coarse-grained hypersolvus granite (T3) to form a tabular sheet corresponding to the upper level of the complex. Renewed subsidence marks a change in the chemistry with the intrusion beneath T3 of a metaluminous hypersolvus granite (T4) followed by a subsolvus granite (T5) displaying low outward-dipping

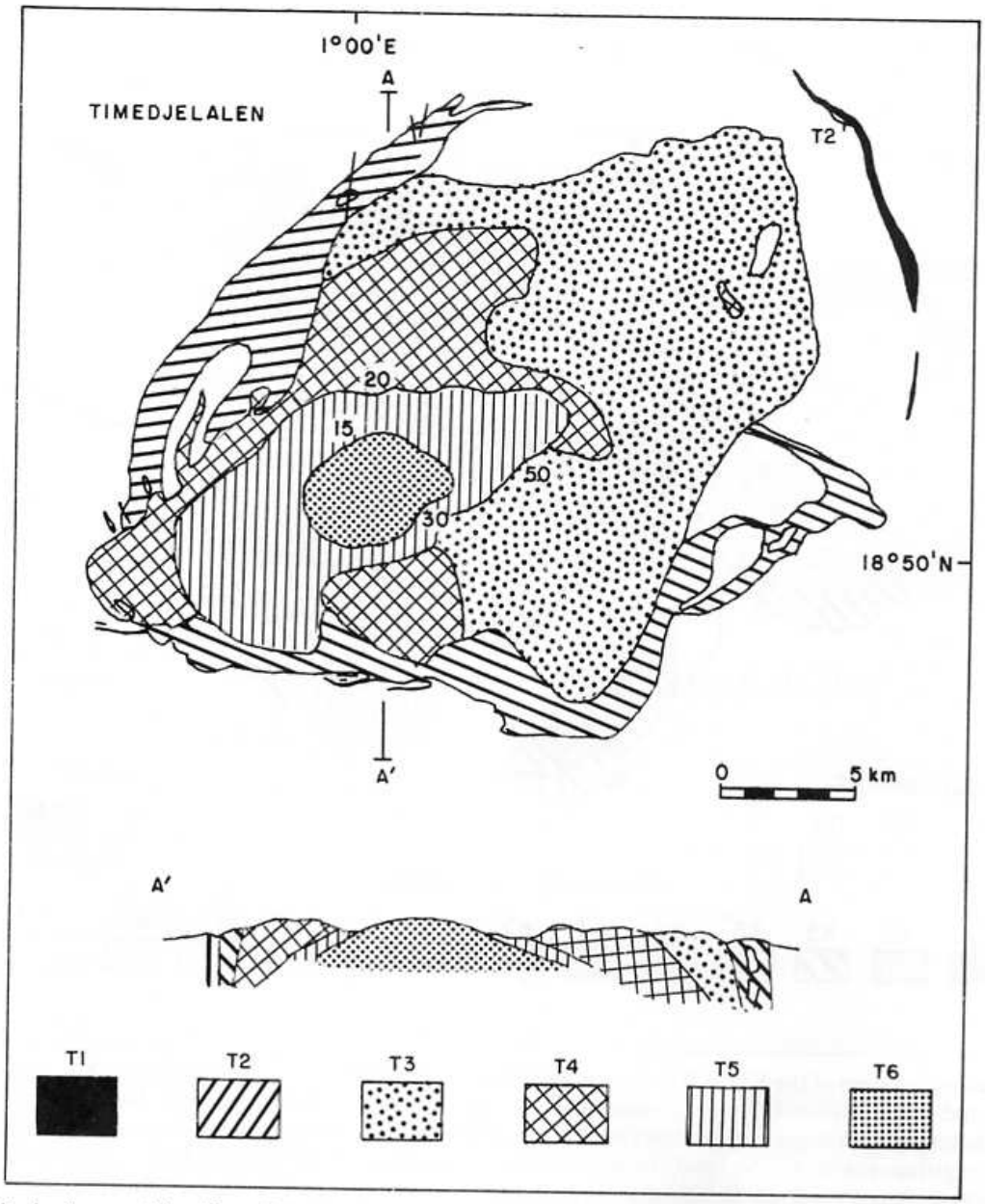

FIG. 5. Geological map of the Timedjelalen ring-complex: T1, granite porphyry; T2, medium-grained granite (perthite, aegirine–augite, Ca-Na- amphibole, biotite); T3, coarse-grained granite (perthite, aegirine–augite, Ca-Na- and Na-amphiboles); T4, heterogranular granite (perthite, oligoclase, amphibole, biotite); T5, fine-grained granite (perthite, oligoclase, biotite); T6, fine- to medium-grained granite (aegirine, arfvedsonite). (Ba *et al.* 1985.)

contacts. Lastly, a peralkaline medium-grained hypersolvus granite (T6) occurs, piercing T5 as a shallow dome.

Despite the mineralogical diversity, the compositional range of the Iforas alkaline province is very narrow. All the rocks are rich in silica with values of 64%–68% for the quartz syenites and 72%–79% for the granites. CaO and MgO are always low, and are reflected by sodic plagioclase (maximum An_{15}) and by mafic minerals with high FeO/(FeO + MgO): fayalite, pyroxenes (Fe-augite, hedenbergite and aegirine), amphiboles (Fe-hornblende, Fe-richterite and arfvedsonite) and Fe-biotite. K_2O (4.2%–5.6%) and Na_2O (3.4%–4.1%) are not particularly high for granites. In molecular proportion, Na_2O is generally slightly in excess of K_2O. The rocks are mainly peralkaline or metaluminous with rare peraluminous varieties containing less than 1% of normative corundum. Fluorine is always abundant but, characteristically, boron is very low and tourmaline is absent. Contents of Th, Zr, Y, Rb and the rare-earth elements (REE) are high, particularly in the peralkaline facies.

Petrologically, the most striking features of the quartz syenites and granites is the abundance of perthites displaying a wide range of textures and the rich assemblage of ferromagnesian minerals

often displaying beautiful reactions and mantling relationships. Ba *et al.* (1985) have shown the presence of two distinct trends.

1 A *sodic peralkaline trend* extends as an evolving fractionation sequence from a metaluminous quartz syenite, characterized by a miaskitic sequence in which the mafic minerals (fayalite, Fe-augite, Ca-amphibole and biotite) crystallize earlier than the K-feldspar and quartz, to peralkaline granite where the Ca-Na- and Na-amphiboles and aegirine are late and mould the feldspars. Relict fayalite is only present in the less-differentiated metaluminous syenite and granite; it is frequently altered and mantled by Ca-amphibole. Clinopyroxenes are nearly always present and form an apparently continuous suite: Fe-augite–hedenbergite–Na-hedenbergite–aegirine. Within a single intrusion, Ca- and Ca-Na-pyroxenes are early and separated from late Na-pyroxenes by the crystallization of amphiboles. Amphiboles show a very wide range in composition. The green Ca-amphiboles have compositions between hornblende, edenite and barroisite and mantle the fayalite and Ca-pyroxene. The blue-green amphiboles mantling the Ca-amphiboles in some of the metaluminous granite and occurring as the main amphiboles in the peralkaline granite range from between barroisite and richterite to arfvedsonite and may be rimmed by riebeckite. Micas are not frequent and are represented by Mg-biotite in the syenites, biotite–annite in the metaluminous granites and lepidomelane in the peralkaline granites. Other typical peralkaline minerals present in the province are aenigmatite and astrophyllite. The accessory minerals include coarse zircon, zoned allanite, Fe-Ti oxides, apatite, fluorite, stilpnomelane and tchevkinite. Sphene is rare in the Kidal complex but is abundant in the Timedjelalen. The albite–microcline–arvfedsonite granite present in the Kidal complex (K12) has undergone strong albitization by sub-solidus alteration of the pre-existing magmatic feldspars and is similar to those described in Nigeria (Jacobson *et al.* 1958).

2 A *potassic-aluminous trend* is represented by granite porphyries, hypersolvus amphibole–biotite granite, subsolvus amphibole–biotite and biotite–chlorite granite. Anhydrous early-formed mafic minerals (fayalite, clinopyroxene) are rare and the ferromagnesian reaction series is much more limited. The calcic amphiboles belong to the hastingsite–actinolite series and are generally euhedral. They are mantled by biotite (annite–lepidomelane) which contains inclusions of zircon, allanite, apatite, Fe–Ti oxides and sphene. Late alteration plays an increasing role on passing from the hypersolvus granite to the subsolvus granite with the appearance of fluorite–albite–chlorite–epidote + muscovite.

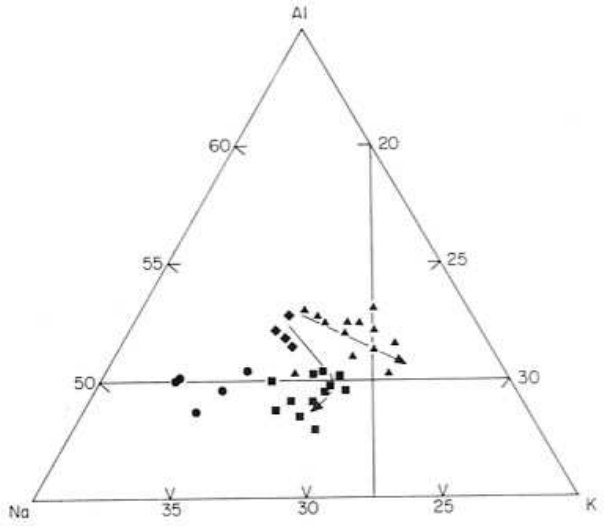

FIG. 6. Na–K–Al (atomic) diagram for the Kidal massif; ♦, syenites; ■, peralkaline hypersolvus granites; ● peralkaline albitized granites; ▲, metaluminous granites. (Ba *et al.* 1985.)

The trends appear clearly on the Na–K–Al diagram (Fig. 6). The evolution from metaluminous quartz syenite to peralkaline granite, passing through transitional facies with fayalite, hedenbergite and Ca–Na-amphiboles, occurs with an increasing (Na + K)/Al ratio and a constant K/Na ratio; after moving into the peralkaline field the K/Na ratio decreases. This path can be explained by a plagioclase effect accompanied by fractionation of early mafic minerals (fayalite, Ca-pyroxene and amphiboles), which is followed by intense fractionation of K-feldspar (orthoclase effect) as it crosses into the peralkaline field and descends the thermal valley (Bailey & Macdonald 1969). This stage may be followed by deuteric recrystallization in the presence of hydrothermal F-bearing fluids giving rise to a sub-trend characterized by a high (K + Na)/Al ratio and a fall in the K/Na ratio corresponding to the albitization of the K-feldspars which produced the albite–microcline–arfvedsonite granite. The aluminous trend from granite porphyries to subsolvus biotite–chlorite granite is marked by decrease of (Na + K) and Na/K ratios. This reflects the appearance of biotite and of perthites with K greater than Na. A possible explanation may be the fractionation of basic oligoclase, Fe-hornblende and clinopyroxene if the dark inclusions sometimes encountered are cumulates.

The independence of the two trends is suggested by the Sr and Ba concentrations. The metaluminous granite porphyries have more Sr (100 ppm) and less Ba (500–800 ppm) than the

syenites (50 ppm Sr, 1000 ppm Ba). This suggests a divergent evolution before the syenite stage, with the common source perhaps being of monzonitic composition. These trends are very similar to those described by various workers in Nigeria, Niger, Corsica, Sudan and New Hampshire, and also occur in mixed oversaturated and undersaturated provinces which may be in continental (Gardar, Quebec, Oslo) or oceanic (Kerguelen) areas. These were first reviewed over 40 years ago by Barth (1944).

To conclude, the Iforas alkaline province displays all the main petrological and geochemical characteristics of typical anorogenic oversaturated alkaline provinces. When compared with the Nigerian province (Jacobson *et al.* 1958; Bowden & Turner 1974) and the Niger province (Black 1963; Black *et al.* 1967), the main differences can be summarized as follows.

1 The volcanism is fissural and the ring-complexes do not appear to have acted as central volcanoes.

2 Basic rocks (gabbros, anorthosites) are absent. It should be noted, however, that gravity data suggests that dense rocks may be present at depth (Ly *et al.* 1984) and some microgabbros have been observed as dykes.

3 Economic mineralization is absent. Among the metaluminous granites, subsolvus varieties are abundant whereas the hypersolvus facies predominate in Niger–Nigeria where the albitized granites are associated with Sn-bearing greisens and contain columbite.

The Pan-African orogenic context

The Iforas alkaline ring-complexes and associated dyke-swarms lie within the Pan-African belt 100–150 km to the E of the suture between the two palaeo-continents, the W African craton and the Tuareg shield. They are aligned N–S along the axis of the composite calc-alkaline batholith of western Iforas, which is a major structural unit bound by N–S mega-shears (Fig. 1). Clearly, an understanding of the alkaline rocks and of the rapid switch from calc-alkaline to alkaline magmatism must take into account Pan-African orogenic evolution.

Detailed mapping of the segment of the batholith between the Kidal ring-complex (latitude 18°00′) and the Tiralrar plateau (latitude 19°30′) (see Figs 2 and 3) has established the relative chronology of magmatic events in this area. The granitoids fall into four groups: (1) low-K calc-alkaline pre-tectonic; (2) high-K calc-alkaline late-tectonic; (3) high-K calc-alkaline post-tectonic; (4) alkaline post-tectonic.

All groups cut the tillite-bearing Tafeliant volcano-sedimentary group whose age can be bracketed between 693 ± 7 Ma (U–Pb age from the granodiorite beneath the base of the Tafeliant group (Caby & Andreopoulos-Renaud 1985)) and 615 ± 5 Ma (U–Pb on zircon from the cross-cutting Adma granodiorite (Ducrot *et al.* 1979)).

Detailed petrographic descriptions of the different massifs have recently been published (Liégeois & Black 1984), and they can be summarized as follows.

(1) The pre-tectonic group is represented by the Erecher tonalite composed essentially of zoned andesine, quartz, green biotite and hornblende, and accessory microcline, sphene, Fe-Ti oxides and zircons. The massif has been mylonitized to variable degrees, locally producing a pronounced foliation and partial recrystallization in high greenschist facies. Some granite plutons (Yenchichi 1 type) may also belong to the pre-tectonic group.

(2) The late-tectonic group is by far the more important in volume and is composed of three major rock types.

(a) The granodiorites, the Adma pluton being typical, display two crystallization steps: the first (quartz, andesine, microcline, green biotite, hornblende, $\pm$clinopyroxene, $\pm$orthopyroxene) is locally affected by the E–W compression producing N–S foliation, whereas the second (amphibole, biotite, quartz–feldspar symplektites) is not affected and is post-tectonic.

(b) The porphyritic monzogranites are composed of slightly perthitic microcline phenocrysts, quartz, oligoclase, green biotite and amphibole, abundant accessory sphene and apatite, Fe-Ti oxides, zircon and secondary chlorite and epidote. They also often display a planar fabric with strong gradients of deformation developed in proximity to shear zones.

(c) The fine-grained monzogranites are composed of millimetre-sized quartz, oligoclase, slightly perthitic microcline, chloritized biotite and accessory sphene, Fe-Ti oxides, allanite, apatite and zircons, and present only a weak planar fabric. Intrusion has followed the porphyritic monzogranite closely, with contact zones often being hybrid and characterized by the presence of large K-feldspar xenocrysts.

(3) The post-tectonic calc-alkaline group is represented by dense WNW–ESE dyke-swarms (Yenchichi and Telabit) and circular sharp-cutting syenogranite plutons. The dykes comprise intermediate to acid rocks (55%–77% SiO_2) and

some of them have alkaline affinities (Dohendal dyke-swarm). The plutons are undeformed, homogeneous in composition and more acid than the preceding groups (Yenchichi 2 pluton).

(4) The late post-tectonic alkaline group includes the Tahrmert granite, spectacular N–S dyke-swarms (quartz syenite porphyries, granophyres, quartz–feldspar porphyries and rhyolites), extrusive rhyolites and ignimbrites (Tiralrar), and high-level ring-complexes (Kidal, Timedjelalen) composed of quartz microsyenites and metaluminous and peralkaline granites.

Ages, isotopic and main geochemical characteristics of the calc-alkaline–alkaline transition

The Rb–Sr system gives for the pre-tectonic family a rehomogenization age which corresponds to the collision event (602 ± 13 Ma, 0.70590 ± 0.0008, 9 whole-rock samples (WR), MSWD = 1.0) (Fig. 7).

The two Rb–Sr isochrons on the Adma granodiorite and on the Aoukenek fine-grained monzogranite (late-tectonic family) give similar ages around 595 Ma with relatively low initial ratios (Adma: 595 ± 24 Ma, 0.70482 ± 0.00026, 9 WR, MSWD = 0.7; Aoukenek: 591 ± 18 Ma, 0.7035 ± 0.0005, MSWD = 0.9) (Fig. 7). As a U–Pb zircon age of 615 ± 5 Ma has been obtained for the Adma pluton (Ducrot *et al.* 1979), the slightly younger Rb–Sr ages are believed to date final consolidation marked by the second stage of crystallization and to correspond to the end of the collision. The porphyritic monzogranite only yields an errorchron, probably owing to the wide scatter of sampling. As its age, on the field evidence can be assumed to be almost contemporaneous with the fine-grained monzogranite, its initial ratio can be bracketed between 0.7042 and 0.7053.

Three dyke-swarms (Yenchichi, Dohendal and Telabit) and one granite pluton (Yenchichi 2) of the post-tectonic calc-alkaline family have been dated using the Rb–Sr method. This group seems to show an age trend from S (Yenchichi swarm: 565 ± 14 Ma, 0.7048 ± 0.0005, 7 WR, MSWD = 4.6; Yenchichi 2 pluton: 577 ± 14 Ma, 0.7038 ± 0.0010, 7 WR, MSWD = 1.6) to N (Dohendal swarm: 558 ± 10 Ma, $0.705\,11 \pm 0.00012$, 7 WR, MSWD = 0.7; Telabit swarm: 544 ± 12 Ma, 0.70505 ± 0.00010, 13 WR, MSWD = 4.6) (Fig. 7). All the representatives of this group also have low initial $^{87}Sr/^{86}Sr$ ratios with values between 0.7038 and 0.7051.

Representatives of the alkaline group, on field evidence, are all younger than the calc-alkaline intrusions. The truncation by the Timedjelalen ring-complex of the transcurrent fault cutting the Takellout and Kidal complexes indicates S–N migration (Figs 2 and 3). The geochronological data confirm the post-tectonic age trend from S to N: S, Kidal ring-complex (561 ± 7 Ma, 0.7061 ± 0.0007, 25 WR MSWD = 2.1); N, Tahrmert pluton (542 ± 7 Ma, 0.7061 ± 0.0004, 12 WR, MSWD = 3.6), N–S dykes (543 ± 9 Ma, 0.7050 ± 0.0003, 14 WR, MSWD = 2.0) and Timedjelalen ring-complex (546 ± 7 Ma, 0.7058 ± 0.0003, 21 WR, MSWD = 3.3) (Fig. 7). In the N all the intrusions are contemporaneous, within the ± 7 Ma limit of error, but the relative chronology established by the field relationships is as follows: 1, Tarhmert; 2, N–S dykes and lavas; 3, Timedjelalen. All the alkaline units have Sr initial ratios between 0.7050 and 0.7060.

The NW–SE sinistral transcurrent faulting has been dated. Such a fault cutting the Yenchichi 2 pluton also affects a part of the earlier Yenchichi 1 pluton. An isochron based on Yenchichi 1 mylonites gives an age around 545 Ma and can be interpreted as the rehomogenization of the Rb–Sr system during the shearing process (544 ± 16 Ma, 0.7063 ± 0.0005, MSWD = 1.6, 9 WR) (Fig. 7).

A geochemical evolution, related to age and tectonic setting, can be traced from the calc-alkaline pre-tectonic group through the late-tectonic and post-tectonic calc-alkaline groups to the alkaline post-tectonic magmatism. This appears on the simple SiO_2 versus $Na_2O + K_2O$ diagram (Fig. 8(a)). Three trends are clearly distinguished: low-K calc-alkaline represented by the pre-tectonic granitoids, a high-K calc-alkaline trend by late- and post-tectonic groups and an alkaline trend for late post-tectonic granites. The distinction between the three trends also appears in other geochemical diagrams, for example in the Rb versus K_2O diagram (Fig. 8(b)). In this diagram, the alkaline group is dispersed perpendicular to Shaw's main trend (Shaw 1968) as in the case of the Rallier du Baty ring-complex in the Kerguelen archipelago (Lameyre *et al.* 1976; Vidal *et al.* 1979). However, the pre- and late-tectonic calc-alkaline families follow the main trend, although with some higher K_2O/Rb ratios. It is interesting to note that the calc-alkaline post-tectonic group shows some alkaline affinities. Several samples of the peralkaline phases of the Timedjelalen ring-complex follow the now classical 'pegmatitic-hydrothermal' trend (Shaw 1968), probably in response to post-magmatic auto-metamorphic fluids (Vidal *et al.* 1979).

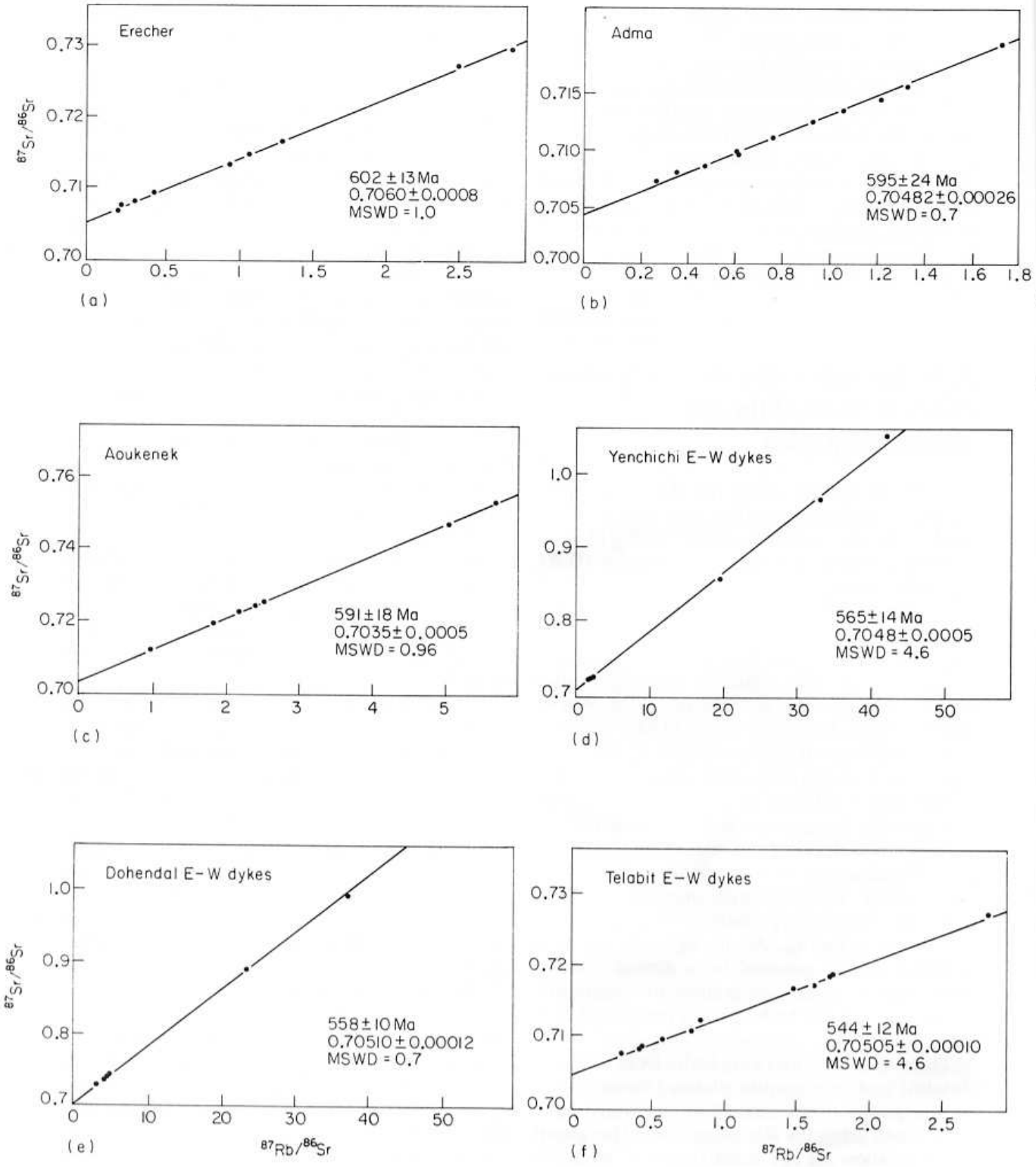

FIG. 7. Rb–Sr isochrons: (a) rehomogenized pre-tectonic Erecher tonalite; (b) late-tectonic Adma granodiorite; (c) late-tectonic Aoukenek monzogranite; (d) post-tectonic Yenchichi E–W dyke-swarm; (e) post-tectonic Dohendal E–W dyke-swarm; (f) post-tectonic Telabit E–W dyke-swarm; (g) post-tectonic Yenchichi 2 circular syenogranite; (h) post-tectonic Tahrmert alkaline granite; (i) post-tectonic alkaline N–S dyke-swarm; (j) post-tectonic Timedjelalen ring-complex; (k) post-tectonic Kidal ring-complex (some samples with very high Rb/Sr ratios are outside the figure (see Liégeois & Black 1984); (l) pre-tectonic (?) Yenchichi 1 granite. Analysed mylonitized samples indicate rehomogenization during late transcurrent faulting events. The calculations were made following Williamson (1968) with $\lambda = 1.42 \times 10^{-11}$ a^{-1}. The errors are at the 2σ level. (From Liégeois & Black 1984.)

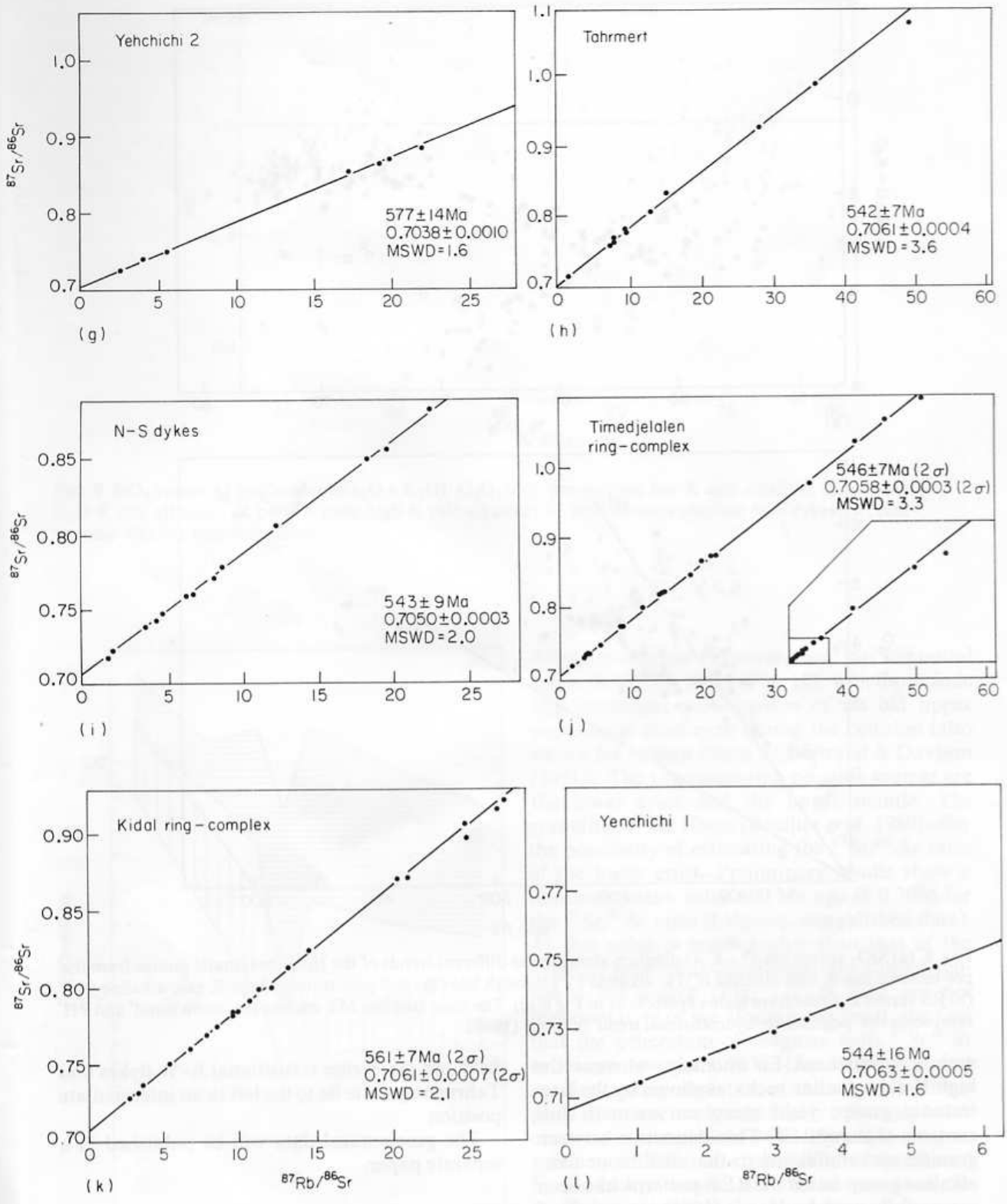

In the alkaline ring-complexes the associated subsolvus metaluminous granites are mineralogically practically indistinguishable from the post-tectonic acid members of the high-K calc-alkaline group. They may be discriminated, however, in the SiO_2 versus agpaitic index (AI) diagram (Fig. 9), the limit between the two groups corresponding to an AI of 0.88. In a REE chondrite-normalized diagram (Fig. 10) (Liégeois & Hertogen, unpublished data) the alkaline group including the metaluminous granites displays a general enrichment in REE, particularly in heavy REE,

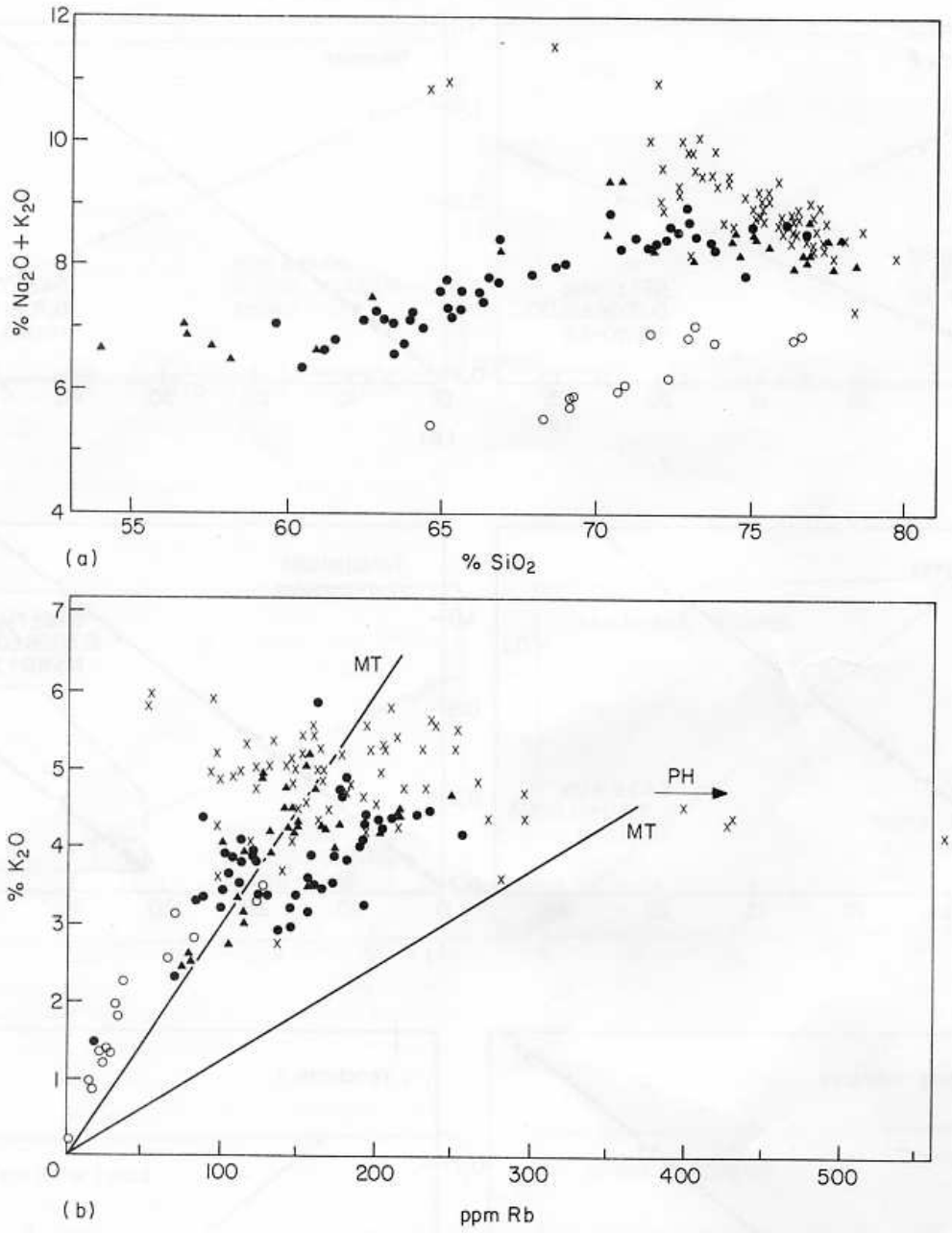

FIG. 8. (a) SiO_2 versus Na_2O+K_2O diagram showing the different trends of the Iforas magmatic groups from the pre-tectonic low-K calc-alkaline (○) to alkaline (×) through late (●) and post-tectonic high-K calc-alkaline (▲); (b) Rb versus K_2O diagram (same symbols as in Fig 8(a)). The lines labelled MT enclose the 'main trend' and PH represents the 'pegmatitic–hydrothermal trend' of Shaw (1968).

with a pronounced Eu anomaly, whereas the high-K calc-alkaline rocks, as shown by the late-tectonic group, yield steep curves with low contents of heavy REE. This distinction between granitic rocks affiliated to the alkaline or calc-alkaline group based on REE patterns has been successfully used by Harris (1985) in a study of mixed anorogenic complexes in Saudi Arabia. The four groups plot distinctly on the Rb against Yb + Ta discrimination diagram (Fig. 11) (Pearce *et al.* 1985). Whilst the pre-tectonic group clearly falls in the VAG field, the late-tectonic granitoids lie astride the VAG and syn-COLG join; the main alkaline representatives plot in the WPG field and the earlier transitional E–W dykes and Tahrmert granite lie to the left in an intermediate position.

The geochemical data will be published in a separate paper.

Interpretation and the petrogenetic model

Three distinct trends, low-K calc-alkaline, high-K calc-alkaline and alkaline, are easily distinguishable in the field and in the laboratory and can be related to successive palaeo-environments.

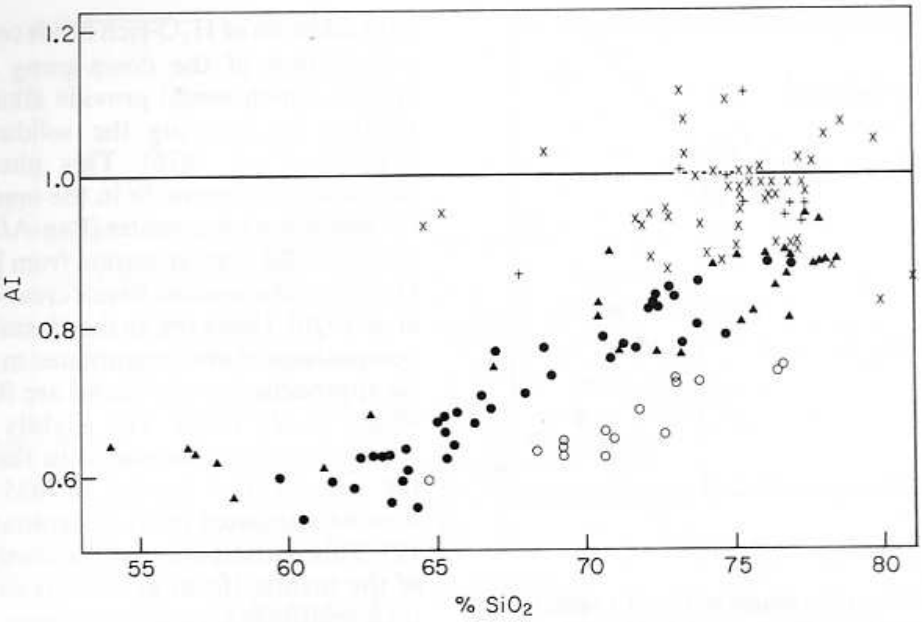

FIG. 9. SiO_2 versus AI (molecular $(Na_2O+K_2O)/Al_2O_3$): ○, pre-tectonic low-K calc-alkaline; ●, late-tectonic high-K calc-alkaline; ▲, post-tectonic high-K calc-alkaline; +, post-tectonic alkaline N–S dykes; ×, post-tectonic alkaline ring-complexes.

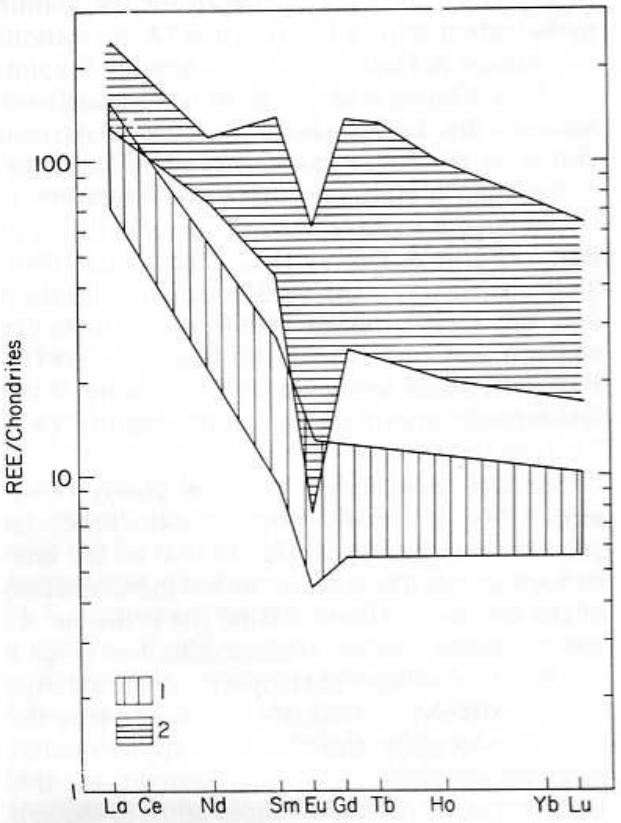

FIG. 10. Range of chondrite-normalized REE for (1) the late-tectonic high-K calc-alkaline group (six samples) and (2) the post-tectonic alkaline group including metaluminous and peralkaline samples (six samples). Data from Liégeois & Hertogen, unpublished.)

All the groups have relatively low $^{87}Sr/^{86}Sr$ initial ratios (0.7035–0.7061) (Fig. 12), which preclude any important participation of an old upper continental crust even during the collision (also shown for eastern Iforas by Bertrand & Davison (1981)). The two remaining possible sources are the lower crust and the upper mantle. The granulites of the Iforas (Boullier *et al.* 1980) offer the possibility of estimating the $^{87}Sr/^{86}$ Sr ratio of the lower crust. Preliminary results show a minimum mean value 600 Ma ago of 0.7066 for the $^{87}Sr/^{86}Sr$ ratio (Liégeois, unpublished data). As this value is much higher than that of the magmas produced, these granulites cannot represent the source (Fig. 12). If they are not representative of the Iforas lower crust, the fact that the generation of magmas with $^{87}Sr/^{86}Sr$ ratios as low as 0.7035 (Aoukenek granite) requires strong depletion of the source in lithophile elements, implying a highly refractory lower crust, is incompatible with abundant magma production. This non-crustal origin is confirmed by the lack of crustal-derived inclusions in the studied plutons.

In contrast, the island arc situated west of the batholith and composed essentially by basic and intermediate rocks reflects the composition of the depleted mantle under the Iforas in Pan-African times and provides homogeneous $^{87}Sr/^{86}Sr$ initial ratios between 0.7025 and 0.7030 (Caby *et al.*, 1986). It would therefore appear that the Iforas

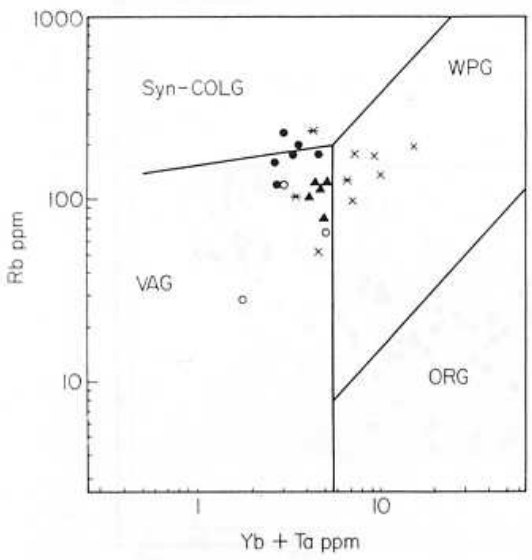

FIG. 11. Discrimination diagram Yb + Ta against Rb (field boundaries from Pearce *et al.* 1985): ○, pre-tectonic low-K calc-alkaline; ●, late-tectonic high-K calc-alkaline; ▲, post-tectonic high-K E–W dykes; *, post-tectonic Tahrmert pluton; ×, post-tectonic alkaline N–S dykes and ring-complexes; VAG, volcanic-arc granite; syn-COLG, syn-collision granite; WPG, within-plate granite; ORG, ocean ridge granite. See text for discussion. (Data from Liégeois & Hertogen, unpublished)

calc-alkaline granitoids have been generated in the mantle with crustal contamination during their ascent. The generation of important amounts of granitic rocks in the mantle has been discussed for many years, the main problem being the need to have at least an equal quantity of basic rocks at depth. In this connection it must not be forgotten that the great crustal thickness in the Andean cordillera (up to 70 km (James 1971) is due not to compression but essentially to vertical accretion from the underlying mantle (Brown 1977). In Western Iforas E–W crustal shortening across the volcano-sedimentary sequences related to the 600 Ma collision has been estimated at only about 65% (Ball & Caby 1984) and probably much less than in the granitoids (Liégeois & Black 1984). It is likely that the mountain building in the Iforas has been due, at least in part, to vertical accretion under the continent in both the subduction and the collision epochs.

If we accept this origin for the Iforas granitoids at mantle depth, several classical models for andesite generation are available (Best 1975; Fyfe & McBirney 1975; Thorpe *et al.* 1976). The most plausible model is probably partial melting in the upper mantle above the subduction zone with addition of H_2O-rich fluids coming from the dehydration of the down-going oceanic lithosphere, which would provide alkalis and favour melting by lowering the solidus temperature (Thorpe *et al.* 1976). This phenomenon can introduce radiogenic Sr in the mantle because of the alteration by seawater (Pan-African $^{87}Sr/^{86}Sr$ around 0.708; extrapolation from Peterman *et al.* (1970)) of the oceanic basalt crust (Hawkesworth *et al.* 1979). However, in the Iforas the Sr isotopic composition of uncontaminated mantle melts can be approached in the island arc (0.7025–0.7030) (Caby *et al.*, 1986). The slightly higher values which have been measured in the cordillera for the calc-alkaline groups (0.7035–0.7051) must then be attributed to crustal contamination (Fig. 12). This participation of the crust in the genesis of the mantle Iforas granitoids can also explain their relatively high silica contents.

In conclusion, we propose for the subduction- and collision-related calc-alkaline rocks a common origin in the mantle with subducted oceanic crust participation and some crustal contamination during the magma ascent (Fig. 13). A main difference between the pre- and late-tectonic magmas is their K_2O (and Rb) contents. This can be explained by a greater depth for the mantle mobilization during the collision (*K–h* relation) (Dickinson & Hatherton 1967; Arculus & Johnson 1978; Dupuy *et al.* 1978). In fact the collision between the Tuareg shield and the W African craton *in the Iforas* has consisted of 'docking' rather than a Himalayan-type confrontation as would appear to have been the case further S in Benin (Burke & Dewey 1972; Trompette 1980). This would explain the weak crustal mobilization and the total absence of S-type granites (in contrast with the Himalayan leucogranites (Le Fort 1981)) and weak syn-COLG affinity of the late-tectonic granitoids in the Rb against Yb + Ta diagram (Fig. 11).

The last calc-alkaline group is poorly represented and is clearly post-tectonic. Since its geochemistry is very similar to that of the late-tectonic group, it is taken as the last manifestation of the source mobilized during the collision. As some samples display alkaline affinities (Figs 8 and 9), a beginning of participation of the alkaline source is likely, particularly in the N where the two post-tectonic families are approximately contemporaneous. The emplacement of this group occurred during the rapid uplift of the belt (Fig. 13).

The Iforas alkaline rocks follow the calc-alkaline post-tectonic group without a significant time break towards the end of the uplift. Indeed, only the early alkaline Tahrmert pluton was eroded during the unroofing of the batholith. This

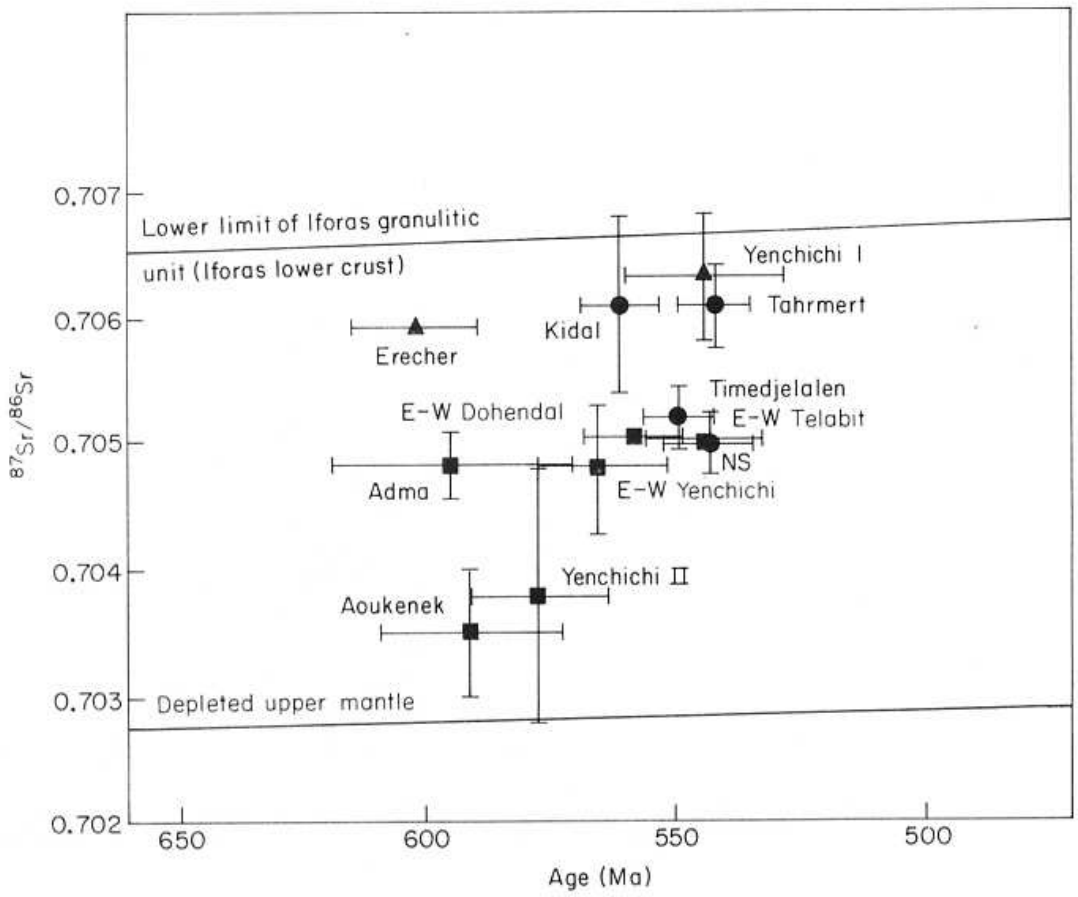

FIG. 12. $^{87}Sr/^{86}Sr$ initial ratios of the intrusions as a function of their isochron age (the error bars represent 2 σ level isochron errors): ▲, pre-tectonic low-K calc-alkaline plutons (rehomogenized values); ■, late- and post-tectonic high-K calc-alkaline plutons and dykes (end-of-crystallization values); ●, post-tectonic high-level alkaline plutons and dykes (intrusion values). The $^{87}Sr/^{86}Sr$ ratio of the Iforas lower crust is inferred from the Iforas granulitic unit and that of the depleted mantle from the island arc (see text).

implies that the lava plateaux, fed by the N–S dyke-swarms, represent relics of a thick volcanic cover which extended over most of the Iforas and under which the ring-complexes were intruded. Volumetrically, the alkaline magmatism was very important, as is confirmed by the rhyolitic and ignimbritic composition of the molasse associated with the belt (Fabre 1982). The onset of alkaline magmatism was accompanied by reactivation of N–S mega-shear zones related to a change in the direction of major constraints shown by the switch in strike in the dyke-swarms from WNW–ESE (calc-alkaline) to N–S (alkaline). Movements along sinistral NNW–SSE transcurrent faults has been dated around 545 Ma (Yenchichi I mylonites). A 560–535 Ma age range based on U–Pb zircon and $^{39}Ar/^{40}$ Ar ages has been obtained from deformed granite within the nearby mega-shear zone defining the western limit of the Iforas granulite unit (Fig. 1) (Lancelot *et al* 1983). Distension, produced essentially by horizontal movements, was weak and marked by narrow grabens filled with molasse located along major shear zones Fabre (1982).

The geochronological data seem to indicate the diachronous emplacement of the two post-tectonic families (from S, 580–560 Ma, to N, 550–540 Ma). This could be related to differences in the rate of uplift which may possibly be linked to the obliquity of the collision (Ball & Caby 1984).

The sudden and radical change in post-tectonic conditions from typical subduction and collision-related calc-alkaline magmatism to alkaline magmatism, displaying all the geochemical and petrological characteristics of within-plate anorogenic complexes, implies the tapping of a new source. Trace-element and REE patterns indicate a less depleted water-poor mantle origin in contrast with a subduction-related source. Pb isotope data on feldspars (Liégeois & Lancelot, unpublished data) show that the calc-alkaline group had a source distinct from the more radiogenic source for the alkaline rocks. The Iforas alkaline ring-complexes have slightly

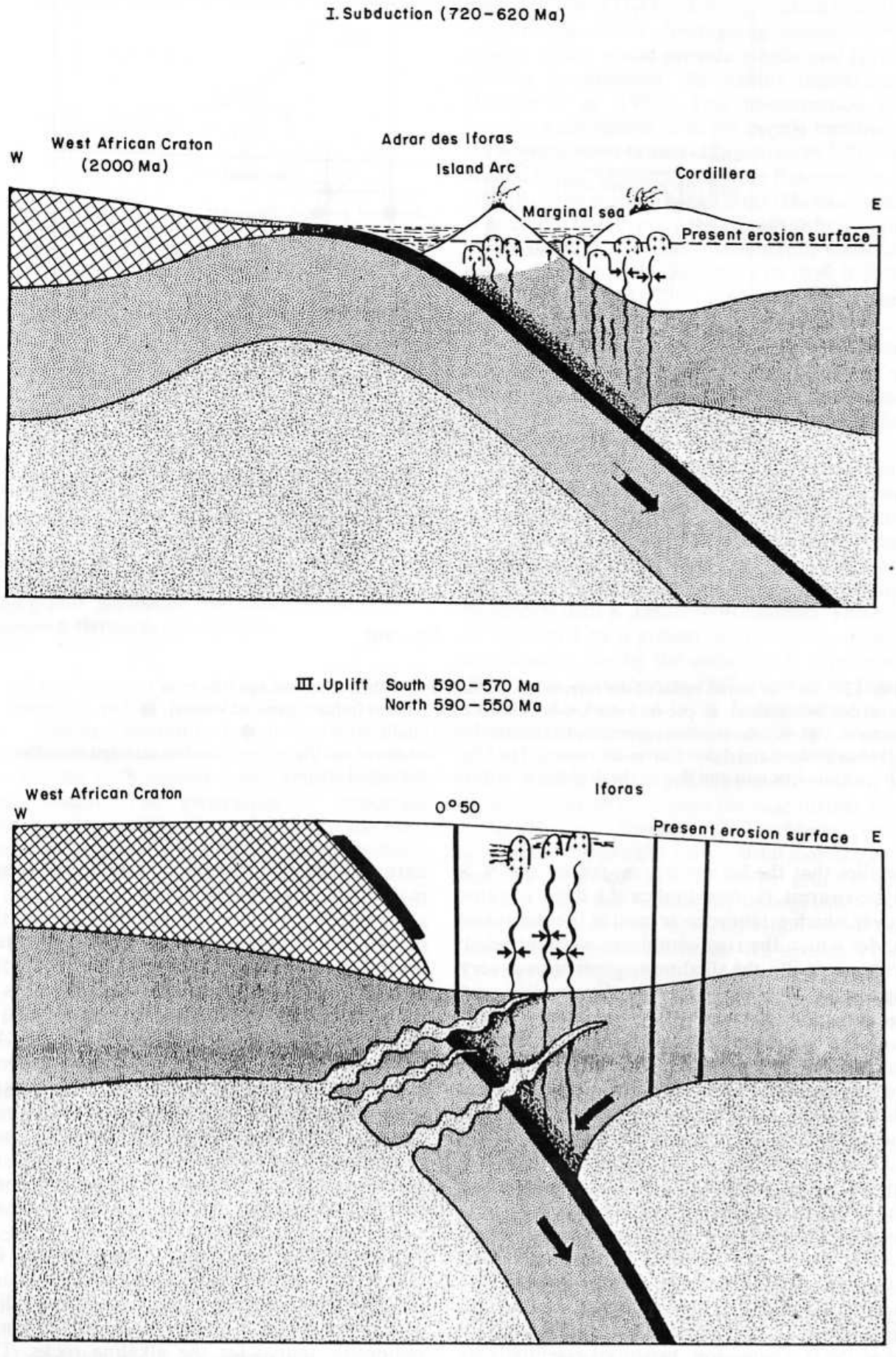

FIG. 13. Schematic representation of the proposed model for the Pan-African magmatic evolution of the Iforas.

II. Collision (620 – 590 Ma)

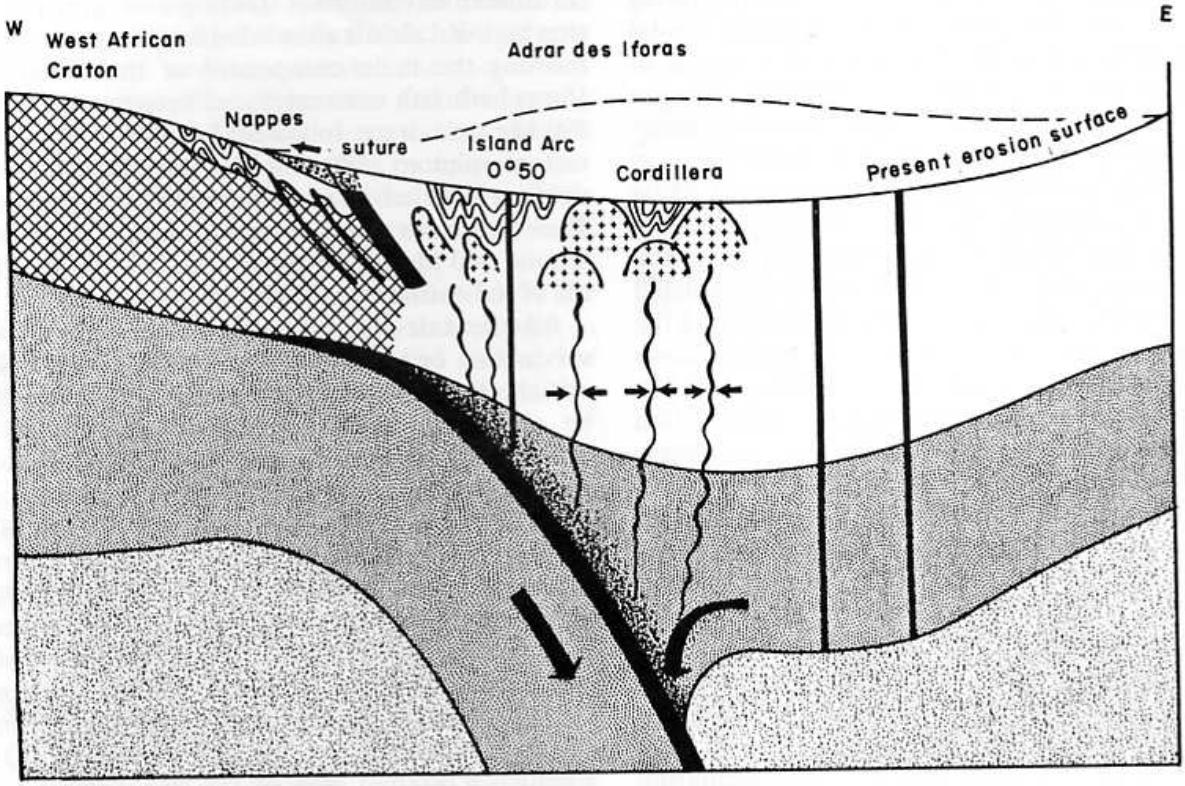

IV. Weak Distension + Transcurrent Movements

South 570
North 550 → ?(max. 500 Ma)

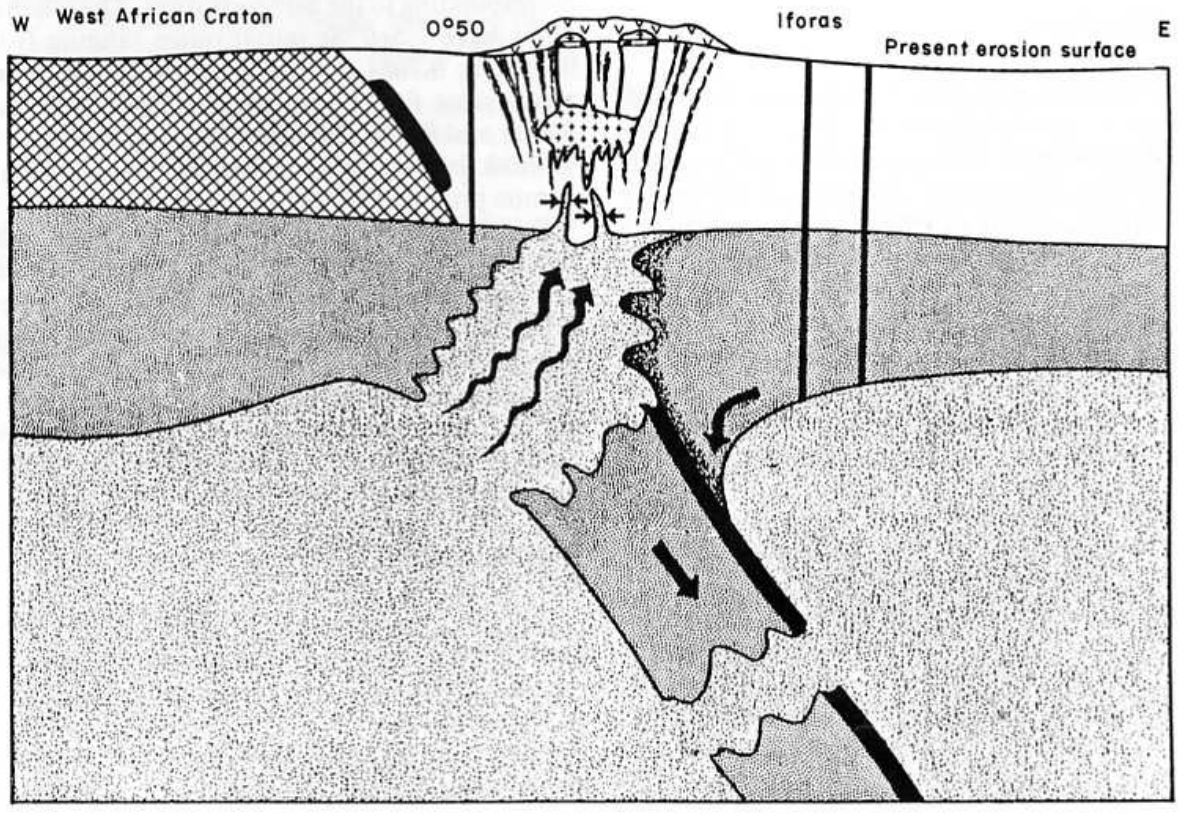

higher $^{87}Sr/^{86}Sr$ initial ratios (0.7050–0.7061) than those of the components of the surrounding calc-alkaline batholith. This precludes crustal contamination at shallow depth as a means of raising the initial ratios. Moreover, oxygen isotope data have shown interaction with meteoric water to have been only very local (Weis *et al.*). Some participation of lower crust is likely but it is difficult to see why it should have been greater than in the case of the calc-alkaline group.

We suggest that the new source is less depleted asthenospheric mantle, originally underlying the subducted plate, which has risen to shallow depth after rupture of the cold plunging plate (Fig. 13). This source would then be the same as that often proposed for within-plate alkaline complexes emplaced in a strictly anorogenic environment. In the case of the nearby Tadhak alkaline undersaturated and carbonatite province of Permian age (Liégeois *et al.* 1983), the main ring-complex (Tadhak) can be interpreted as a pure mantle product on the basis of Sr and Pb isotopic data (Weis & Liégeois 1983) with a source of the ocean island basalt type. An estimation of the Sr isotopic composition of this deep mantle in Pan-African times can be obtained by calculating back the isochron-deduced $^{87}Sr/^{86}$ Sr initial ratio to 550 Ma. This gives a ratio of about 0.7043, which is clearly distinct from that of the depleted lithospheric mantle represented by the island-arc lavas (0.7025–0.7030).

Conclusions

The Cambrian oversaturated alkaline province, with its extrusive plateau rhyolites, spectacular acid dyke-swarms and typical alkaline 'younger-granite' ring-complexes, displays all the major petrographical and geochemical characteristics of anorogenic within-plate magmatism, despite its appearance only a few million years after a major orogeny (Pan-African) and its location along a sutured convergent plate boundary. As the magmatic products are essentially the same in contrasting settings, the source must be identical and an explanation for peculiarities must be sought in the basement geology (Black *et al.* 1985).

There is now considerable evidence for interpreting the Pan-African Trans-Saharan orogenic belt (Cahen *et al.* 1984) in terms of a Wilson cycle ending with collision between the passive continental margin of the W African craton and the active margin of the Tuareg shield around 620 Ma (Black *et al.* 1979; Caby *et al.* 1981). In the Iforas, subduction-related low-K calc-alkaline pre-tectonic magmatism is recorded in the interval 725–620 Ma and is found in both an island-arc and a cordilleran environment. During and after collision high-K calc-alkaline late-tectonic granitoids forming the main component of the Western Iforas batholith were emplaced between 620 and 590 Ma and were followed by affiliated post-tectonic plutons (580–550 Ma) during the rapid uplift which led to unroofing of the batholith. The switch to alkaline magmatism occurred around 560 Ma ago in the S and 545 Ma ago in the N indicating a northward migration.

All the calc-alkaline magmatism related to subduction or to collision present low $^{87}Sr/^{86}Sr$ initial ratios between 0.7035 and 0.7051 and may be related to a lithospheric depleted mantle source with participation of subducted oceanic crust at depth and lower-crust Eburnean granulites during ascent. The island-arc material suggests that this mantle source has had an $^{87}Sr/^{86}Sr$ initial ratio around 0.7025–0.7030 (Caby *et al.*, 1986). The absence of typical crustal granites (S-type) is probably due to the oblique nature of the collision which in the Western Iforas did not lead to a doubling of the crust as in the Himalayan situation. These results, in contrast with W. Q. Kennedy's original view of the Pan-African as an episode of basement reactivation (Kennedy 1964), provide strong evidence of important crustal accretion during this event.

The switch to alkaline magmatism with its distinctive geochemical characteristics is attributed to a different more primitive mantle source corresponding to the asthenosphere. The alkaline rocks have $^{87}Sr/^{86}Sr$ initial ratios ranging from 0.7050 to 0.7061 compared with an estimated mean value for this source of 0.7043, based on Rb–Sr and Pb–Pb data from the nearby Permian Tadhak undersaturated complex which is a pure mantle product (Weis & Liégeois 1983).

Structurally, the onset of alkaline magmatism in the Iforas occurred at the end of major uplift and was accompanied by a change in the stress field with renewed and intermittent transcurrent movements along lithospheric mega-shear zones and related wrench faults producing distension, as indicated by the presence of dyke-swarms and narrow molasse-filled grabens. In the model proposed, access to a new source is explained by rise of the asthenosphere to shallow depths beneath continental lithosphere after rupture of the cold subducted plate.

Asthenospheric mantle, which has often been considered as a source for alkaline magmatism, takes into account the petrological and geochemical features common to all A-type granites. It can be argued that differences such as the presence or absence of associated tin mineralization are due to the nature of the country rocks. The

chances of finding economic Sn deposits are considerably enhanced when the intrusions cut crustally derived granitoids which have already redistributed and concentrated the metal, e.g. Nigerian Pan-African granites and tin-bearing pegmatites. In the Iforas, where the basement is composed of depleted granulitic rocks and essentially mantle-derived granitoids, there is little possibility of finding such mineralization (Black 1984).

Lastly, we would like to stress that whilst the source of alkaline magmatism is to be sought in the deep mantle, its location and nature are largely controlled by the structure, composition and dynamics of the overlying continental lithosphere (Black *et al.* 1985).

ACKNOWLEDGEMENTS:
This work is a result of collaboration between the Direction Nationale de la Géologie et des Mines, Mali, the Centre Géologique et Géophysique, Montpellier, the Laboratoire de Pétrologie, Paris VI, and the Musée Royal de l'Afrique Centrale, Tervuren. We acknowledge the financial support of the FNRS and Ministère de l'Education Nationale of Belgium and of the CNRS and Fond d'Aide et de Coopération of the French Republic.

References

ARCULUS, R. J. & JOHNSON, R. W. 1978. Criticism of generalised models for the magmatic evolution of arc-trench systems. *Earth planet. Sci. Lett.* **39**, 118–26.

BA, H., BLACK, R., BENZIANE, B., DIOMBANA, D., HASCOET-FENDER, J., BONIN, B., FABRE, J. & LIÉGEOIS, J. P. 1985. La province des complexes annulaires sursaturés de l'Adrar des Iforas, Mali. *J. Afr. Earth Sci.* **3**, 123–42.

BAILEY, D. K. & MACDONALD, R. 1969. Alkali–feldspar fractionation trends and the derivation of peralkaline liquids. *Am. J. Sci.* **267**, 242–48.

BALL, E. & CABY, R. 1984. Open folding and constriction synchronous with nappe tectronics along a mega-shear zone of Pan-African age. *In*: KLERKX, J. & MICHOT, J. (eds) *Géologie africaine—African Geology*, pp. 75–90. Musée Royal de l'Afrique Centrale, Tervuren.

BARTH, T. F. W. 1944. Studies on the igneous rock complex of the Oslo region. II. Systematic, petrography of the plutonic rocks. *Skr. Norsk. Vitensk.-Akad. Oslo I*, **9**, 1–104.

BAYER, R. & LESQUER, A. 1978. Anomalies gravimétriques de la bordure orientale du craton ouest-africain: géométrie d'une suture pan-africaine. *Bull. Soc. géol. Fr.* **20**, 863–76.

BERTRAND, J. M. L. & DAVISON, I. 1981. Pan-African granitoïds emplacement in the Adrar des Iforas mobile belt (Mali). A Rb–Sr isotope study. *Precambr. Res.* **14**, 333–62.

BEST, M. G. 1975. Migration of hydrous fluids in the upper mantle and potassium variation in calc-alkalic rocks. *Geology*, **3**, 429–32.

BLACK, R. 1963. Note sur les complexes annulaires de Tchouni-Zarniski et de Gouré (Niger). *Bull. Bur. Rech. geol. minière*, **1**, 31–45.

—— 1984. The Pan-African event in the geological framework of Africa. *Pangea*, **2**, 8–16.

——, CABY, R., MOUSSINE-POUCHKINE, A., BAYER, R., BERTRAND, J. M. L., BOULLIER, A. M., FABRE, J. & LESQUER, A. 1979. Evidence for Precambrian plate tectonics in West Africa. *Nature, Lond.* **278**, 223–7.

——, JAUJOU, M. & PELLATON, C. 1967. Notice explicative de la carte géologique de l'Aïr à l'échelle 1/500 000. *Dir. Mines Géol., Niamey, Niger*

——, LAMEYRE, J. & BONIN, B. 1985. The structural setting of alkaline complexes *J. Afr. Earth Sci.* **3**, 5–16.

BONIN, B. 1980. Les complexes acides alcalins anorogéniques continentaux: l'exemple de la Corse. *Thèse Etat*, Université de Paris VI (unpublished).

BOULLIER, A. M., DAVISON, I., BERTRAND, J. M. L. & COWARD, M. 1980. L'unité granulitique des Iforas: une nappe de socle d'âge Pan-Africain précoce. *Bull. Soc. géol. Fr.* **20**, 877–82.

BOWDEN, P. & TURNER, D. C. 1974. Peralkaline and associated ring-complexes in the Nigeria–Niger province, West Africa. *In:* SØRENSEN, H. (ed.) *The alkaline rocks*, pp. 330–51. Wiley, London.

BROWN, G. C. 1977. Mantle origin of cordilleran granites. *Nature, Lond.* **265**, 21–4.

BURKE, K. & DEWEY, J. F. 1972. Orogeny in Africa. *In*: DESSAUVAGIE, T. F. J. & WHITEMAN, A. J. (eds.) *African Geology*, pp. 583–608. Ibadan University Press, Ibadan.

CABY, R. 1970. La chaîne pharusienne dans le nord-ouest de l'Ahaggar (Sahara central, Algérie); sa place dans l'orogenèse du Précambrien supérieur en Afrique. *Thèse Etat*, Université de Montpellier.

—— 1980. Les nappes précambriennes du Gourma dans la chaîne pan-africaine du Mali. Comparaison avec les Alpes occidentales. *Rev. Géogr. phys. Géol. dyn.* **21**, 365–76.

—— 1981. Associations volcaniques et plutoniques prétectoniques de la bordure de la chaîne pan-africaine en Adrar des Iforas (Mali): un site de type arc-cordillère au Protérozoïque supérieur. *11th Colloq. on African Geology, Milton Keynes*, p. 30.

—— & ANDREOPOULOS-RENAUD, U. 1985. Etude pétrostructurale et géochronologique d'une métadiorite quartzique de la chaîne pan-africaine de l'Adrar des Iforas (Mali). *Bull. Soc. Géol. Fr., Sér 8*, **1**, 899–903.

——, BERTRAND, J. M. L. & BLACK, R. 1981. Pan-African ocean closure and continental collision in the Hoggar-Iforas segment, central Sahara. *In*: KRÖNER, A. (ed.) *Precambrian Plate Tectonics*, pp. 407–34. Elsevier, Amsterdam.

CABY, R., LIÉGEOIS, J. P., DOSTAL, C., DUPUY, C. & ANDREOPOULOS-RENAUD, U. 1986. The Tilemsi arc and the Pan-African suture zone in Northern Mali. *Int. Field Conf. Proterozoic Geology and Geochemistry (IGCP 215–17)*, Colorado, USA, p. 88.

CAHEN, L., SNELLING, N. J., DELHAL, J. & VAIL, J. R. 1984. *The Geochronology and Evolution of Africa*, 512 pp. Clarendon Press, Oxford.

CHIKHAOUI, M. 1981. Les roches volcaniques du Protérozoïque supérieur de la chaîne pan-africaine du NW de l'Afrique (Hoggar, Anti-Atlas, Adrar des Iforas). Caractérisation géochimique et minéralogique—implications géodynamiques. *Thèse Etat*, Université de Montpellier.

DICKINSON, W. R. & HATHERTON, T. 1967. Andesitic volcanism and seismicity around the Pacific. *Science*, **157**, 801–3.

DUCROT, J., DE LA BOISSE, H., RENAUD, U. & LANCELOT, J. 1979. Synthèse géochronologique sur la succession des événements magmatiques pan-africains au Maroc, dans l'Adrar des Iforas et dans l'est du Hoggar. *10e Colloq. de Géologie d'Afrique, Montpellier*, p. 40.

DUPUY, C., DOSTAL, J. & VERNIERES, J. 1978. Genesis of volcanic rocks related to subduction zones, geochemical point of view. *Bull. Soc. géol. Fr.* **19**, 1233–44.

DUYVERMANN, H. J., HARRIS, N. B. W. & HAWKESWORTH, C. J. 1982. Crustal accretion in the Pan-African: Nd and Sr evidence from the Arabian shield. *Earth planet. Sci. Lett.* **54**, 315–26.

EATON, G. P. 1982. The Basin and Range province, origin and tectonic significance. *Annu. Rev. Earth planet. Sci.* **10**, 409–40.

FABRE, J. 1982. Pan-African volcano-sedimentary formations in the Adrar des Iforas. *Precambr. Res.* **19**, 201–14.

——, BA, H., BLACK, R., CABY, R., LEBLANC, M. & LESQUER, A. 1982. La chaîne pan-africaine, son avant-pays et la zone de suture au Mali. *Notice explicative de la carte géologique et gravimétrique de l'Adrar des Iforas au 1/500 000*, Bamako, Mali.

FYFE, W. S. & MCBIRNEY, A. R. 1975. Subduction and the structure of andesitic volcanic belts. *Am. J. Sci.* **275A**, 285–97.

HARRIS, N. B. W. 1982. The petrogenesis of alkaline intrusives from Arabia and northeast Africa and their implications for within-plate magmatism. *Tectonophysics*, **83**, 243–58.

—— 1985. Alkaline complexes from the Arabian shield. *J. Afr. Earth Sci.* **3**, 83–8.

HAWKESWORTH, C. J., NORRY, M. J. RODDICK, J. C. & BAKER, P. E. 1979. $^{143}Nd/^{144}Nd$, $^{87}Sr/^{86}Sr$, and incompatible element variations in calc-alkaline andesites and plateau lavas from South America. *Earth planet. Sci. Lett.* **42**, 45–57.

INNOCENTI, F., MAZZUOLI, R., PASQUARE, G., RADICATI DI BROZOLO F. & VILLARI, L. 1982. Tertiary and Quaternary volcanism of the Erzurum kars area (Eastern Turkey). Geochronological and geodynamic evolution. *J. Volcanol. geotherm Res.* **13**, 223–40.

JACOBSON, R. R. E., MACLEOD, W. N. & BLACK, R. 1958. Ring-complexes in the Younger Granite province of northern Nigeria. *Mem. geol. Soc. Lond.* **1**, 1–72.

JAMES, D. E. 1971. Plate tectonic model for the evolution of the Central Andes. *Geol. Soc. Am. Bull.* **82**, 3325–46.

KENNEDY, W. Q. 1964. The structural differentiation of Africa in the Pan-African (±500 m.y.) tectonic episode. *Res. Inst. Afr. Geol. Univ. Leeds, 8th Annu. Rep.*, pp. 48–9.

LAMEYRE, J., MAROT, A., ZIMINE, S., CANTAGREL, J. M., DOSSO, L. & VIDAL, P. 1976. Chronological evolution of the Kerguelen islands syenite–granite ring-complex. *Nature, Lond.* **263**, 306–7.

LANCELOT, J. R., BOULLIER, A. M., MALUSKI, H. & DUCROT, J. 1983. Deformation and related radiochronology in a late Pan-African mylonite bearing shear zone, Adrar des Iforas, Mali. *Contrib. Mineral. Petrol.* **82**, 312–26.

LE FORT, P. 1981. Manaslu leucogranite: a collision signature of the Hymalaya. A model for its genesis and emplacement. *J. geophys. Res.* **16**, 10 545–68.

LIÉGEOIS, J. P. & BLACK, R. 1984. Pétrographie et géochronologie Rb–Sr de la transition calco-alcaline—alcaline fini-pan-africaine dans l'Adrar des Iforas (Mali): accrétion crustale au Précambrien supérieur. *In*: KLERKX, J. & MICHOT, J. (eds.) *Géologie Africaine—African Geology*, pp. 115–45. Musée Royal de l'Afrique Centrale, Tervuren.

——, BERTRAND, H., BLACK, R., CABY, R. & FABRE, J. 1983. Permian alkaline undersaturated and carbonatite province, and rifting along the West African craton. *Nature, Lond.* **305**, 42–3.

LOISELLE, M. C. & WONES, D. R. 1979. Characteristics and origin of anorogenic granites. *Abstracts 92nd G.S.A. and Annu. Meet.* **11**, 468.

LY, S., LESQUER, A., BA, H. & BLACK, R. 1984. Structure profonde du batholite occidental de l'Adrar des Iforas (Mali): une synthèse des données gravimétriques et géologiques. *Rev. Géogr. phys. Géol. dyn.* **25**, 33–44.

MOUSSINE-POUCHKINE, A. & BERTRAND-SARFATI, J. 1978. Le Gourma: un aulacogène du Précambrien supérieur? *Bull. Soc. géol. Fr.* **20**, 851–6.

PEARCE, J. A. HARRIS, N. B. W. & TINDLE, A. G. 1985. Trace element discrimination diagrams for the tectonic interpretation of granitic rocks. *J. Petrol.* **25**, 956–83.

PETERMAN, Z. E., HEDGE, C. E. & TOURTELOT, H. A. 1970. Isotopic composition of strontium in seawater throughout Phaneorozoic time. *Geochim. cosmochim Acta*, **34**, 105–20.

SAUVAGE, J. F. & SAVARD, R. 1985. Les complexes alcalins sous-saturés à carbonatites de la région d'In Imanal (Sahara malien): une présentation. *J. Afr. Earth Sci.* **3**, 83–8.

SHAW, D. M. 1968. A review of K–Rb fractionation trends by covariance analysis. *Geochim. cosmochim Acta*, **32**, 573–601.

THORPE, R. S., POTTS, P. J. & FRANCIS, P. W. 1976. Rare earth data and petrogenesis of andesite from the north Chilean Andes. *Contrib. Mineral. Petrol.* **54**, 65–78.

TROMPETTE, R. 1980. La chaîne pan-africaine des Dahomeyides et le bassin des Volta (bordure SE du craton ouest-africain). *In*: BESSOLES, B. (ed.) *Géologie de l'Afrique : la Chaîne Pan-Africaine, Zone Mobile d'Afrique Centrale (Partie Sud) et Zone Mobile Soudanaise, Mem. Bur. Rech. Géol. Min. Fr.* **92**, 11.

VIDAL, P., DOSSO, L., BOWDEN, P. & LAMEYRE, J. 1979. Strontium isotope geochemistry in syenite–alkaline granite complexes. *In*: AHRENS, L. H. (ed.) *Origin and Distribution of the Elements*, pp. 223–31. Pergamon Press, Oxford.

WEIS, D. & LIÉGEOIS, J. P. 1983. U–Pb whole rock isochron in the Tadhak ring-complex (Mali). Petrogenetic implications. *Int. Conf. on Alkaline Ring-complexes*, p. 36. Zaria and Jos, Nigeria.

WEIS, D., LIÉGEOIS, J. P. & BLACK, R. Tadhak alkaline ring complex (Mali): existence of U–Pb isochrons and 'Dupal' signature 270 Ma ago. *Earth planet. Sci. Lett.* in press.

WILLIAMSON, J. H. 1968. Least-square fitting of a straight line. *Can. J. Phys.* **46**, 1845–7.

J. P. LIÉGEOIS, Service de Géochronologie, Musée Royal de l'Afrique Centrale, 1980 Tervuren, Belgium.

R. BLACK, Laboratoire de Pétrologie, CNRS-UA728, Université P. et M. Curie, 75230 Paris Cedex 05, France.